Contents lists available at ScienceDirect

Solid State Communications

Communication

Optimization of exchange bias in Co/CoO magnetic nanocaps by tuning deposition parameters

CrossMark

A. Sharma[a,*], J. Tripathi[b], K.C. Ugochukwu[c], S. Tripathi[a,1]

[a] Department of Physics, Manipal University Jaipur, Jaipur, India
[b] Department of Physics, ISLE, IPS Academy, Indore, India
[c] Department of Physics, Federal University of Technology, PMB 1526 Owerri, Imo-State, Nigeria

A R T I C L E   I N F O

A B S T R A C T

In the present work, we report exchange bias tuning by varying thin film deposition parameters such as synthesis method and underlying layer patterning. The patterned substrates for this study were prepared by self-assembly of polystyrene (PS) latex spheres (~530 nm) on Si (100) substrate. The desired magnetic nanocaps composed of CoO/Co bilayer film on these patterned substrates were prepared by molecular beam epitaxy technique under ultra-high vacuum conditions. For this, a Co layer of ~10 nm thickness was deposited on the substrates and then oxidized in-situ to form CoO/Co/PS in-situ oxidized film or ex-situ in ambiance which also gives CoO/Co/PS naturally oxidized film. Simultaneously, reference thin films of Co (~10 nm) were also prepared on plane Si substrate and similar oxidation treatments were performed on them respectively. The magnetic properties studied using SQUID technique revealed higher exchange bias (~1736 Oe) in the in-situ oxidized Co/PS film as compared to that in naturally oxidized Co/PS film (~1544 Oe) and also compared to the reference film. The observed variations in the magnetic properties are explained in terms of surface patterning induced structural changes of the deposited films and different oxidation methods.

1. Introduction

An important parameter in the study of magnetic nanostructures is the exchange bias phenomenon from both fundamental and technical perspectives [1,2]. The exchange bias effect was first observed in Co(FM)/CoO(AFM) core-shell nanoparticles by Meiklejohn and Bean [3]. The general features of exchange bias effect can be understood by a simple intuitive model and accordingly, the exchange bias phenomenon occurs when a structure containing ferromagnetic (FM) and antiferro-magnetic (AFM) bilayer materials is cooled down through the Néel temperature of the AFM material in an external magnetic field. Above the Néel temperature of AFM, the material behaves like a paramagnetic material, while below this temperature antiferromagnetic order is induced. The applied field during the cooling from above the Néel temperature determines the direction of the freezing of AFM and FM domains. Due to exchange coupling between ferromagnetic and anti-ferromagnetic interfacial spins, an unidirectional anisotropy is induced in the FM layer. As a result, a shift in the hysteresis loop is observed along the direction opposite to that of the cooling magnetic field. In this regard, the interface between Co (FM) and CoO (AFM) is the most widely studied system so far, not only because exchange bias was first

discovered in this system but also because this system provides much higher unidirectional anisotropy than other similar systems [4,5]. CoO has a Neel temperature of 290 K, so exchange bias can easily be reset by just increasing the sample temperature up to room temperature. Secondly, Co forms a mono magnetic AFM oxide unlike Fe whose oxides forms various magnetic phases [6]. This system has been investigated in the form of bilayer, multilayers, nanoparticles, alloys, core-shell system and patterned structures [7–12] and being prepared by various techniques like evaporation, sputtering, clustering and colloidal methods [13–16]. It is well reported that AFM material plays an important role to determine exchange bias properties for example, and its many parameters like thickness, particle size, preparation method strongly influence exchange bias properties [17–20]. Generally, in case of thin films, multilayers, core-shell systems, to induce exchange bias, Co is exposed to oxygen either in-situ or ambient to form CoO on top of Co. However, the effect of variation in oxidation method on the exchange bias properties has not been studied so far in detail and thus, is not fully yet understood. In this study, we have done the oxidation of Co film by two different methods. In the first method, oxidation of Co was done in-situ in a separate chamber just after deposition of Co film. The film prepared by this way is referred to as

* Corresponding author.
    E-mail address: anupamcsr@gmail.com (A. Sharma).
  [1] Current affiliation: Optics And Thin Film Laboratory, Bhabha Atomic Research Centre, Vishakhapatnam, India.

CoO/Co/PS in-situ film throughout this study. However, same set of sample was oxidized by atmospheric oxygen, thus forming CoO/Co bilayered film. The sample prepared in this way was referred to as CoO/Co/PS naturally oxidized sample herein and thereafter. To compare the exchange bias properties, Co films were also deposited on flat Si substrates (referred to as in-situ and naturally oxidized reference film respectively) and similar oxidation treatments were performed on them respectively.

The main motivation of the present study is to investigate the effect of oxidation on the exchange bias in CoO/Co magnetic nanocaps. This "magnetic cap" refers to a magnetic thin film deposited on an array of polystyrene nanospheres. The film is only deposited on the upper hemisphere of the nanospheres and the thickness of the deposited film varies across the nanospheres; from apex to the equator giving the deposited film its 'cap shape'. Because of the variation in thickness, the exchange and dipolar interactions between the spheres are limited. Hence, the film on each nanosphere can be considered as an isolated "magnetic cap" [21]. Due to curvature of nanosphere, the film takes curved shape and grows in curved manner, so obtained magnetic properties are different then the same film deposited on flat substrate in same deposition condition.

We have used nanosphere lithography (also known as natural lithography) to synthesize self-assembled nanospheres. This technique has some unique advantages over other lithographic techniques such as one can control shape of nanostructures, large area uniformity and low cost, which make this technique a nice tool to fabricate very small scale structures [22,23]. Detail understanding of exchange bias in reduced dimension system is essentials for fundamental mechanisms as well as for future magnetic storage devices.

2. Experimental details

An array of polystyrene latex spheres (PS, 530 nm diameter) had been prepared by self-assembly method using nanosphere lithography on Si substrate. Prior to this, the substrates were cleaned in HF solution and then rinsed repeatedly with de-ionized water. Following the substrate preparation, nanospheres solution was drop coated on it and was allowed to dry. In this way, the nanospheres arrange themselves to form two dimensional hexagonally closed packed array on the substrate surface.

The Scanning electron microscopy (SEM) measurements were performed on this PS nanosphere patterned substrate using Philips XL 30 series FEG SEM microscope operated at 10 keV. The image clearly reveals the uniformity of the deposited PS nanospheres over a large area (see Fig. 1). The average size of the nanosphere calculated from the image was found to be ~532 nm. This patterned substrate was then used for a set of Co film (~10 nm thickness) deposition at room temperature by molecular beam epitaxy (MBE) at normal angle deposition geometry under ultra high vacuum (~5×10^{-10} mbar pressure) conditions. For comparison, an identical Co thickness was also
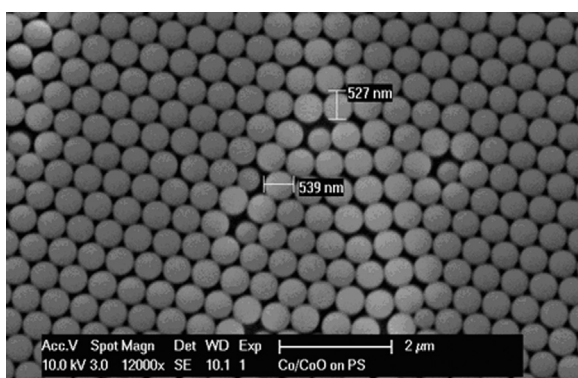
deposited simultaneously on plane (bare) Si substrate. Immediately after deposition, in-situ oxidation of both films was carried out at ~4×10^{-4} mbar oxygen partial pressure for 90 s in an attached but isolated preparation chamber. Another piece from the same set of these samples (Co/PS and Co/Si) was directly exposed to ambient to make CoO from atmospheric oxygen. X-ray reflectivity (XRR) technique was used to characterize the layer structure of the deposited films. These measurements were carried out with Cu Kα wavelength (0.154 nm) on Bruker D8-discover x-ray diffractometer. From the fitting of XRR data, a CoO layer of around ~3 nm on the top of both Co/plane Si substrate oxidized samples was observed. Superconducting quantum interference device (SQUID) magnetization measurements were carried out using a Quantum Design MPMSXL system at low temperature (5 K) on these structures. All the magnetization loops were recorded up to and beyond saturation field of the deposited films. The surface topography was investigated by atomic force microscopy (AFM) technique using Nanoscope dimension 3000 microscope.

3. Results

3.1. XRR and AFM measurements

A model depicting the growth of Co film on both PS nanosphere and Si substrates is shown in Fig. 2 where one can see that the deposited film has grown on each substrate in different manners. In the case of PS nanosphere, the film follows the curvature of underlying nanosphere and hence, on itself grows with a curved surface pattern.

In order to determine the influence of underlying substrate on the structural properties such as thickness, roughness and surface morphology of the deposited films XRR and AFM techniques were employed. The obtained results are shown in Figs. 3 and 4. XRR technique is useful for qualitative as well as quantitative estimation of thickness and roughness of the top surface of the film as well as of the interface between film and substrate. Fig. 3 shows the XRR pattern of naturally oxidized Co film deposited on PS and Si substrates respectively. In case of film deposited on PS substrate, the reflected intensity starts decreasing fast at very low angles and does not show any oscillations or fringes. The absence of any oscillations (Keissig fringes) in this XRR pattern suggests very high roughness of the substrate, as expected in case of polystyrene nanospheres. This roughness in the film arises due to wavy structure of underlying nanosphere, which influences the film growth and hence, the deposited film takes the same curved shape (termed as correlated roughness). On the other hand, XRR pattern of oxidized Co film deposited on Si substrate (naturally oxidized) shows clear appearance of Kiessig fringes (oscillations). These oscillations are known to appear due to the interference of X-rays reflected from various interfaces and their amplitude depends on the electron density contrast between adjacent layers. In case of Co/Si film, the appearance of Kiessig fringes suggests lesser roughness of the film as compared to that in Co/PS film. With the help of Parratt formulism [24,25] we have optimized different parameters such as layer thickness, roughness and electron density to fit the experimental data (fitted data is shown in the Fig. 3 along with the raw data). For this
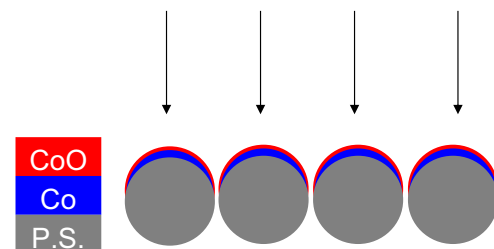

Fig. 1. SEM image of PS (530 nm) nanospheres deposited on Si substrate.

Fig. 2. Schematics of the Co film deposited on plane and modulated polystyrene substrate, which show different growth of film on each substrate.
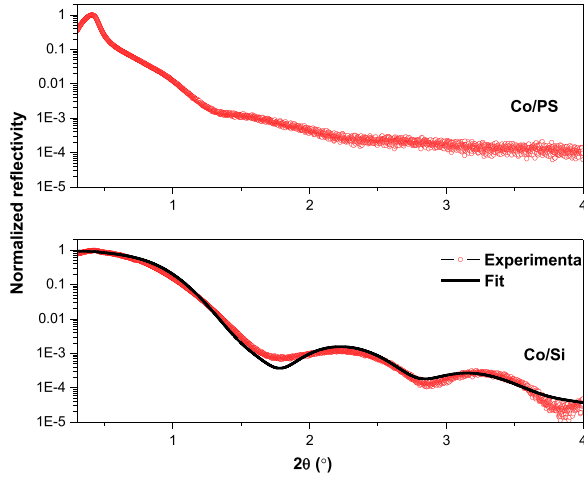
Fig. 3. XRR patterns of naturally oxidized Co/PS and Co/Si film.
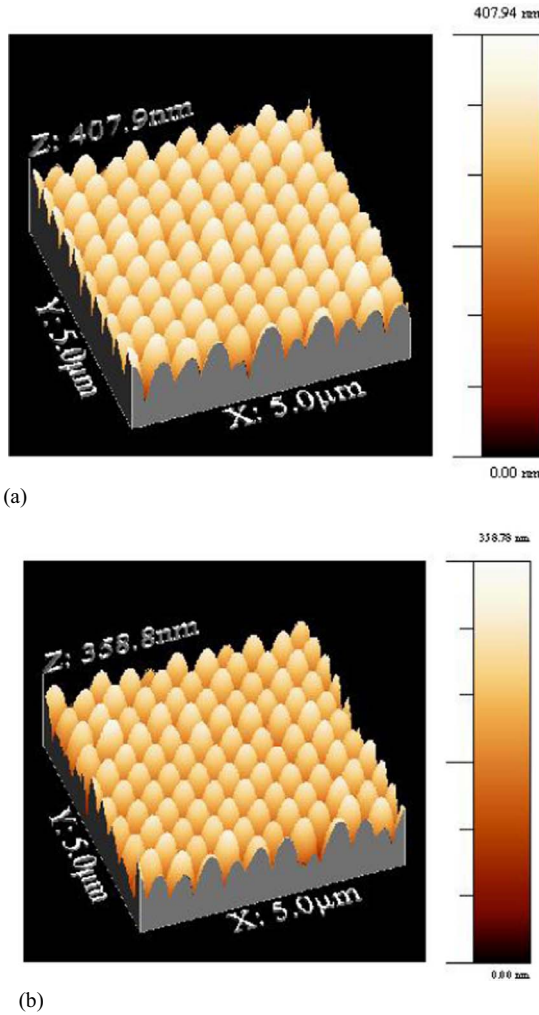

(a)

(b)

Fig. 4. (a) 3D-AFM image of PS nanospheres synthesized on Si substrate. (b) 3D-AFM image of naturally oxidized Co/PS film.

fitting, a layer model was considered which includes a substrate coated with Co film and finally covered with a top layer of CoO. The thicknesses of CoO and Co layer were found to be ~2.8 nm and ~6.5 nm respectively. Similarly, the roughness values of CoO and Co layer were ~0.4 nm and ~0.3 nm respectively. The XRR pattern of Co/PS could not be fitted possibly due to its high roughness (as discussed above).

In order to evaluate the roughness of nanospheres, which could not be obtained from XRR, we have recorded AFM images on nanosphere substrate (prior to Co deposition) and on naturally oxidized Co/PS film. As it is clear from Fig. 4, nanospheres are uniformly arranged in hexagonal closed packed manner, which is retained even after deposition of thin film. The analysis of AFM image corresponding to PS nanosphere array on Si substrate over an area of 5×5 μm^2 (using WSxM 5.0 software) revealed an r.m.s. roughness of ~50.5 nm whereas in case of Co/PS film it was ~47.5 nm. The difference in roughness values in both the samples (before and after deposition of Co) is very small as compared to total roughness. The difference in roughness values obtained from XRR and AFM techniques is due to the different length scale probed by them. XRR averages the roughness over a much larger area as compared to that of AFM, which gives an overall surface topography. As it is clear from the r.m.s. values, roughness decreases slightly after the film deposition but is very high as compared to the film thickness.

3.2. SQUID measurements

Fig. 5 shows the hysteresis loop recorded on such Co films deposited on patterned PS nanosphere and plane substrates subjected to different oxidation methods. All these hysteresis loops were recorded by keeping the applied magnetic field parallel to the sample surface. To study the exchange bias, the samples were cooled down under the action of positive magnetic field of 1.0 T strength.

The exchange bias value was calculated from the graphs using the following relation:

$$(H_{EB}) = [\frac{(H_{left} + H_{right})}{2}]$$ (1)

where, H_{EB} is exchange bias field and H_{left} and H_{right} are the external fields measured on either side of the loop at zero magnetization. Similarly, coercivity values were calculated by the relation:

$$(H_C) = [\frac{(|H_{left}| + |H_{right}|)}{2}]$$ (2)

where H_C is the coercive field. The exchange bias field is determined from the loop shift after subtracting the linear diamagnetic component from the Si substrate. It is clear from the recorded loops that all the samples show a negative exchange bias (i.e. the direction of loop shift is opposite to the direction of applied cooling field, which is positive in the present case). However, the magnitude of exchange bias is different in each case. In-situ oxidized CoO/Co/PS film shows highest exchange bias (−1736 Oe) than the naturally oxidized (−1544 Oe) sample. The exchange bias in the in-situ oxidized sample (CoO/Co/PS) is nearly 2 times higher than that in the corresponding in-situ reference (−803 Oe) sample (CoO/Co/Si). Similarly, the exchange bias in the naturally oxidized CoO/Co/PS sample is much higher (−1540 Oe) than its reference sample (−24 Oe). Along with this, the coercivity in both types of oxidized samples is very large as compared to their reference counterparts. In the in-situ oxidized CoO/Co/PS sample, the coercivity was found to be ~2164 Oe, which is much higher than its reference sample (~943 Oe). Interestingly, naturally oxidized CoO/Co/PS sample shows relatively less coercive field of ~1695 Oe. The naturally oxidized reference sample shows the lowest coercive field among all the studied samples and in this case it was only ~100 Oe.

In addition, all the samples show distinct shapes of hysteresis loops. In-situ oxidized CoO/Co/PS sample shows a step in the descending branch of the hysteresis loop after remanence, which was absent in the ascending branch of the loop where a clear S shaped curve was observed. Corresponding reference sample also shows a step in the descending branch of the loop which was absent in the increasing branch of the loop but the overall shape is different from the samples deposited on polystyrene nanosphere mediated substrate. On the other hand, a less pronounced step can easily be seen (in case of naturally
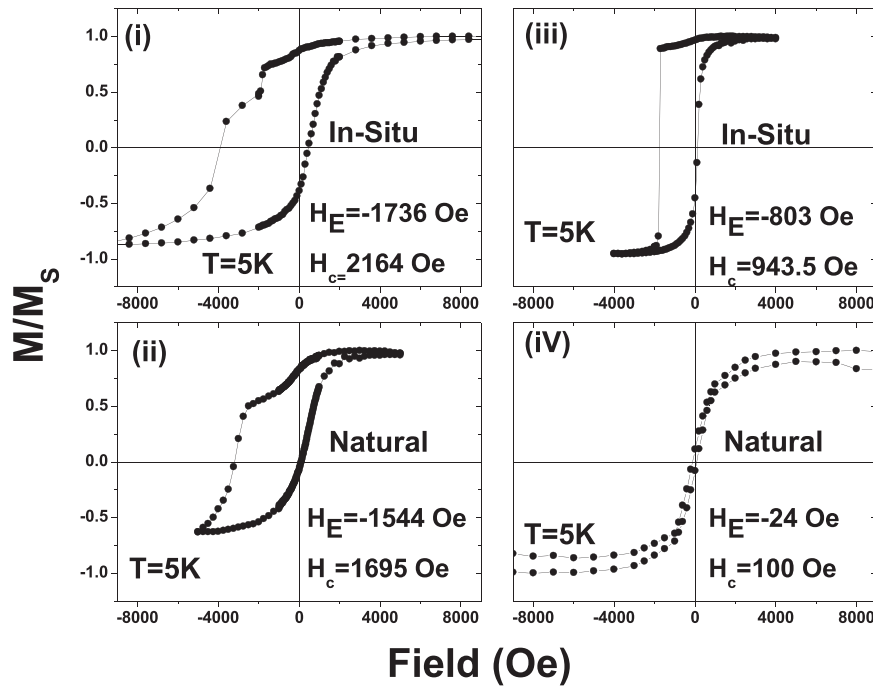
Fig. 5. In-plane field cooled magnetization measurements carried out on (i) CoO/Co/Ps in-situ oxidized, (ii) CoO/Co/PS naturally oxidized, (iii) CoO/Co/Si in-situ oxidized and (iv) CoO/Co/Si naturally oxidized samples.

oxidized CoO/Co/PS sample) in the descending branch of the hysteresis loop whereas a smooth reversal was seen in the increasing branch of the loop. However, corresponding reference loop exhibits a symmetric shape with very low value of remanent magnetization, smallest coercivity and the overall non closed shape of the loop.

4. Discussion

As seen from Fig. 5, a step is clearly visible in the descending branch of all loops except in the case of the naturally oxidized CoO/Co/Si reference sample. This step originates from the Co film deposited on uncovered area i.e. the area in between the adjacent nanospheres. On a closer inspection of the hysteresis loop of in-situ oxidized reference sample, it is observed that this step is also present, however the loop is more straight in this reference sample. The similar trend of this step in both polystyrene mediated substrate sample loops (in-situ oxidized and naturally oxidized samples) also supports the statement about self-assembly. This is the general observation associated with self-assembly process [26−28], that it always results in the inclusion of a lot of defects and dislocations when done in a large area. These films were grown simultaneously with their reference samples, yet they have grown in different manners on PS nanosphere and on Si substrates. Also, their exposure to oxidation was different, thus, it is clear that the observed changes in magnetic properties are not only due to variations in preparation method but also due to curved/plane nature of the underlying substrate in both cases. In case of films grown on nanosphere array, the only factor responsible for different value of exchange bias is the oxidation method. This strong statement stems from the fact that both films were grown on equal sizes of nanospheres, producing equal heights/widths of the curved films.

Here the enhancement of exchange bias on the nanocaps as compared to corresponding reference film is discussed first and in the next step, the influence of oxidation method on the exchange bias is discussed by considering the huge exchange bias observed in both nanocap samples. It is a known fact that at low dimensions, enhancement in exchange bias takes place and this fact is mainly attributed to nanostructuring, simultaneously with the presence of various microstructures [1]. The dependency of exchange bias on various microstructural parameters e.g. grain size and/or roughness has attracted significant attention and a lot of experimental and theoretical studies have been carried out in this direction [29−32]. In this regard, the random field model using pinning effect was proposed which basically deals with the interaction between FM and AFM layers in the presence of interfacial roughness/defects [33]. Li and Zhang further modified this model with the incorporation of finite grain size effect on the coercivity [34]. According to the modified model, due to high AFM anisotropy, the spin flop transition (field-driven reorientation transition) does not occur during hysteresis cycle and the magnetization process is mainly governed by two energy terms, the exchange interaction between FM-FM material and the random field of FM-AFM interfacial material on the FM material. If the interaction between FM-FM is higher, with application of external magnetic field all FM domains are aligned together and in this case FM domains are much larger than the grain size of AFM domains. In this way the random field of FM-AFM material acting on the FM layer is ruled out, resulting in a small enhancement in the coercivity. On the other hand, if the random field is stronger/comparable than FM coupling, the domains of the FM layer grown during magnetization reversal will not be much larger than the grain size. This model mainly relies on the fact that the FM domain size depends on the grain size, which in turn depends on the FM layer thickness. When the thickness is $\leq$ 10 nm (similar to our case) the domain size is comparable to the grain size and therefore the coercivity is larger. The higher exchange bias in our case can be explained within the framework of this model where grain size plays an important role. In the past, it has been experimentally found that 30% variation in film thickness can be observed on different areas of nanospheres [35] and this is also applicable in the present case (also discussed earlier). It results in smaller grain size at the edges leading to more exchange interaction between FM-AFM layers in this region. Thus smaller FM domain size and higher exchange bias field are observed due to small thickness. An inverse relationship between exchange bias and FM thickness ($H_E \propto 1/t_{FM}$) is already reported in the literature, which exhibits that exchange bias is an interface effect. Due to thickness variation on the nanospheres, in particular the low thickness at the mid-rim of the nanosphere, hence, a higher exchange bias is expected in Co/PS film than the reference film [36].

Another important factor which needs attention is the surface/ interface roughness. It is related to thickness as well as grain size because the film deposited on the nanospheres also has a varying roughness since its thickness and also the grain sizes are different at different places due to curvature. The nanospheres also have their own roughness, which also affects the overall roughness of the deposited film to a very large extent. Our experimental observations of corresponding AFM measurements carried out without any deposition and after Co film deposition on these nanospheres also support this statement. In CoO/Co system, exchange bias increases with increase in roughness as also reported in the literature [37–39].

The difference in exchange bias value in both (in-situ and naturally oxidized) samples depends on the oxidation treatment. It has been reported that the film prepared by natural oxidation treatment results a discontinuous layer of oxides while the oxidation carried out by in-situ method results in more homogeneous oxide layer [40]. The discontinuity in oxide layer decreases the total available volume over which the exchange interaction occurs among ferromagnetic domains and affects the magnetization reversal process. Because of this, total random filed averages out to be smaller which increases the size of ferromagnetic domains. This results in the decrease in exchange bias and coercivity in naturally oxidized CoO/Co/PS film.

5. Conclusions

In this work, we have successfully synthesized polystyrene (PS) latex nanospheres (~530 nm) on Si (100) substrate by self-assembly method (using nanosphere lithography). A Co film (10 nm) has been deposited on these spheres using molecular beam epitaxy (MBE) technique. To induce exchange bias, oxidation of Co was done in-situ in a separate chamber just after deposition of Co film. The film prepared by this way was referred to as CoO/Co/PS in-situ film. However, similar piece from the same set of samples was oxidized in atmospheric oxygen, thus forming CoO/Co bilayered film. The sample prepared in this way was referred to as CoO/Co/PS naturally oxidized sample. To compare the exchange bias properties, Co films were also deposited on flat Si substrates (referred to as CoO/Co/Si films) and similar oxidation treatments were performed on them respectively. The observed changes in magnetic properties were attributed to the curvature of the magnetic nanocaps on the polystyrene nanospheres, which results in different growth process different from that on the plane Si reference film. Also, the exchange bias property was affected differently by the different oxidation methods. The observed results provide a method to tune the exchange bias by changing preparation condition which may be useful for both fundamental and technological points of view.

References

[1] (a) J. Nogués, I.K. Schuller, J. Magn. Magn. Mater. 192 (1999) 203;

(b) J. Nogúes, J. Sort, V. Langlais, V. Skumryev, S. Surinach, J.S. Munoz, M.D. Baro, Phys. Rep. 422 (2005) 65;

(c) J.I. Martín, J. Nogués, K. Liu, J.L. Vicent, I.K. Schuller, J. Magn. Magn. Mater. 256 (2003) 449.

[2] A.E. Berkowitz, K. Takano, J. Magn. Magn. Mater. 200 (1999) 552.

[3] W.H. Meiklejohn, C.P. Bean, Phys. Rev. 102 (1956) 1413.

[4] G. Nowak, A. Remhof, F. Radu, A. Nefedov, H.W. Becker, H. Zabel, Phys. Rev. B 75 (2007) 174405.

[5] J.B. Yi, J. Ding, Solid State Phenom. 111 (2006) 175.

[6] D. Tripathy, A.O. Adeyeye, Phys. Rev. B 79 (2009) 064413.

[7] D. Kumar, S. Singh, A. Gupta, J. Appl. Phys. 120 (2016) 085307.

[8] M. Gierlings, M.J. Prandolini, H. Fritzsche, M. Gruyters, D. Riegel, Phys. Rev. B 65 (2002) 092407.

[9] M. Feygenson, E.V. Formo, K. Freeman, N. Schieber, Z. Gai, A.J. Rondinone, J. Phys. Chem. C 119 (2015) 26219.

[10] J.M. Riveiro, J.A. De Toro, J.P. Andrés, J.A. González, T. Muñoz, J.P. Goff, Appl. Phys. Lett. 86 (2005) 172503.

[11] P. Nieves, D. Kechrakos, O. Chubykalo-Fesenko, Phys. Rev. B 93 (2016) 064432.

[12] A. Sharma, S. Tripathi, K.C. Ugochukwu, J. Magn. Magn. Mater. 326 (2013) 97.

[13] U. Lagerqvist, P. Svedlindh, K. Gunnarsson, J. Lu, L. Hultman, M. Ottosson, A. Pohl, Thin Solid Films 576 (2015) 11.

[14] N. Akdogan, A. Yagmur, M. Oztürk, E. Demirci, O. Ozturk, M. Erkovan, J. Magn. Magn. Mater. 373 (2015) 120.

[15] R. Wu, J.Z. Wei, X.L. Peng, J.B. Fu, S.Q. Liu, Y. Zhang, Y.H. Xia, C.S. Wang, Y.C. Yang, J.B. Yang, Appl. Phys. Lett. 104 (2014) 182403.

[16] J.B. Tracy, D.N. Weiss, D.P. Dinega, M.G. Bawendi, Phys. Rev. B 72 (2005) 064404.

[17] J.A. Borchers, Y. Ijiri, S.-H. Lee, C.F. Majkrzak, G.P. Felcher, K. Takano, R.H. Kodama, A.E. Berkowitz, J. Appl. Phys. 83 (1998) 7219.

[18] J.G. Hu, G.J. Jin, Y.Q. Ma, J. Appl. Phys. 94 (2003) 2529.

[19] D. Tripathy, A.O. Adeyeye, J. Appl. Phys. 105 (2009) 07C110.

[20] K.W. Lin, F.T. Lin, Y.M. Tzeng, Z.Y. Guo, Eur. Phys. J. B 45 (2005) 237.

[21] (a) M. Albrecht, G. Hu, I.L. Guhr, T.C. Ulbrich, J. Boneberg, P. Leiderer, G. Schatz, Nat. Mater. 4 (2005) 203;

(b) A. Sharma, S. Tripathi, K.C. Ugochukwu, J. Tripathi, Thin Solid Films 536 (2013) 249–255.

[22] C.L. Hayens, R.P. Van Duyne, J. Phys. Chem. B 105 (2001) 5599.

[23] J.C. Hulteen, R.P. Van Duyne, J. Vac. Sci. Technol. A 13 (1995) 1553.

[24] L.G. Parratt, Phys. Rev. 95 (1954) 359.

[25] C. Braun, PARRATT32-the reflectivity tool, HMI Berlin, 1997.

[26] P. Colson, C. Henrist, R. Cloots, J. Nanomater. 2013 (2013) 19.

[27] T.R. Jensen, M.L. Duval, K.L. Kelly, A.A. Lazarides, G.C. Schatz, R.P. Van Duyne, J. Phys. Chem. B 103 (1999) 9846.

[28] F.J. Szabo, S. Aştilean, Z. Neda, Chem. Phys. Lett. 408 (2005) 241.

[29] E.I. Shanova, I.O. Dzhun, N.G. Chechenin, Inorg. Mater. Appl. Res. 5 (2014) 89.

[30] R. Wu, J.B. Fu, D. Zhou, S.L. Ding, J.Z. Wei, Y. Zhang, H.L. Du, C.S. Wang, Y.C. Yang, J.B. Yang, J. Phys. D Appl. Phys. 48 (2015) 275002.

[31] D.L. Cortie, A.G. Biternas, R.W. Chantrell, X.L. Wang, F. Klose, Appl. Phys. Lett. 105 (2014) 032402.

[32] M. Meinert, B. Büker, D. Graulich, M. Dunz, Phys. Rev. B 92 (2015) 144408.

[33] A.P. Malozemoff, Phys. Rev. B 35 (1987) 3679.

[34] L. Zhanjie, Z. Shufeng, Phys. Rev. B 61 (2000) (R 14897).

[35] M.M. Soares, E. de Biasi, L.N. Coelho, M.C. dosSantos, F.S. De Menezes, M. Knobel, L.C. Sampaio, F. Garcia, Phys. Rev. B 77 (2008) 224405.

[36] G. Malinowski, M. Albrecht, I.L. Guhr, J.M.D. Coey, S. van Dijken, Phys. Rev. B 75 (2007) 012413.

[37] J. Wang, T. Sannomiya, J. Shi, Y. Nakamura, J. Appl. Phys. 113 (2013) 17D707.

[38] J. Wang, T. Sannomiya, J. Shi, Y. Nakamura, J. Appl. Phys. 111 (2012) 07D725.

[39] R.F.L. Evans, D. Bate, R.W. Chantrell, R. Yanes, O. Chubykalo-Fesenko, Phys. Rev. B 84 (2011) 092404.

[40] K. Temst, E. Popova, H. Loosvelt, M.J. Van Bael, S. Brems, Y. Bruynseraede, C. Van Haesendonck, H. Fritzsche, M. Gierlings, L.H.A. Leunissen, R. Jonckheere, J. Magn. Magn. Mater. 304 (2006) 14.